Proceedings of the 28th IEEE
EMBS Annual International Conference
New York City, USA, Aug 30-Sept 3, 2006

In-vivo Measurement of Surgical Needle Intervention Parameters: A Pilot Study

T.K. Podder[1], J. Sherman[1], D. Fuller[1], E.M. Messing[2,4],
D.J. Rubens[3,4,5], J.G. Strang[3,4], R. A. Brasacchio[1], Y. Yu[1,5]
Departments of [1]Radiation Oncology, [2]Urology, [3]Radiology, and [4]Surgery,
University of Rochester Medical Center, Rochester, NY 14642, USA.
[5]Department of Biomedical Engineering,
University of Rochester, Rochester, NY 14642, USA.

Abstract – **Percutaneous intervention is essential in numerous medical diagnostic and therapeutic procedures. In these procedures, accurate insertion of the surgical needle is very important. But precise interstitial intervention is quite challenging. Robot-assisted needle intervention can significantly improve accuracy and consistency of various medical procedures. To design and control any robotic system, the design and control engineers must know the forces that will be encountered by the system and the motion trajectories that the needling mechanism will have to follow. Several researchers have reported needle insertion forces encountered while steering through soft tissue and soft material phantoms, but hardly any *in-vivo* force measurement data is available in the literature. In this paper, we present needle insertion forces and motion trajectories measured during actual brachytherapy needle insertion while implanting radioactive seeds in the prostate glands of twenty five patients.**

I. INTRODUCTION

In low-dose-rate (LDR) prostate brachytherapy, accuracy of the radioactive seeds placement is very important for optimal dose delivery to the targeted tissues sparing the critical organs and structures. In traditional transperineal LDR brachytherapy procedures, the fixed grid holes in the template allow the surgeon to insert the needle at specified fixed positions. Very little can be done to steer the needles to a place other than these specific locations. However, alterations in needle insertion position may be required based on intraoperative planning. Sometimes, especially for larger prostates, the needle needs be angulated to avoid pubic arch interference (PAI) and gain access to the desired target position in the prostate. In the currently practiced brachytherapy with a fixed template, needle angulation is almost impossible, although the surgeon can use a hook to bend the needle and get to the desired position after several trials. To overcome some of the limitations and improve accuracy and consistency in LDR, recently several researchers are developing robotic systems for permanent seed implant (PSI) in the prostate [1]-[3].

To design and control any robotic system, the design engineer must know the robotic workspace, motion profile, and force-torque that will be encountered by the system. Especially for tranperineal prostate brachytherapy procedures, the workspace analysis and the assessment of force-torque encountered by the needle insertion mechanism are critical mainly due to two reasons: (a) the limited space available between two legs of the patient (when on the operating table in lithotomy position) to insert a needle through the perineum, and (b) the needle must penetrate through several layers of different types of tissue (skin, perineal muscles, bulbospongiosus tissue, fascia tissue, prostate capsule, prostate tissue, etc. [4]) which exert variable forces. Therefore, *in-vivo* measurement of needle insertion force is very useful in designing any robotic system that will work in such a constrained space.

Some mechanical properties such as modulus of elasticity (Young's modulus), Poisson's ratio, relaxation, stress and strain, measured from *ex-vivo* human tissues, are available in the literature [5]-[10]. Although *ex-vivo* measurement can be more accurate for a small piece of sample, there are two main differences between *ex-vivo* and *in-vivo* measurements, especially for PSI: (a) during *in-vivo*, i.e. actual brachytherapy in the operating room (OR), the needle traverses through different types of tissues/organs having nonlinear viscoelastic properties, and (b) factors such as the boundary conditions acting on the organ, organ/tissue interface, blood flow, temperature and humidity differences, etc. None of these issues can be resolved accurately using current state-of-the-art methodology and technology. Since these *ex-vivo* experiments are fundamentally different from the needle insertion experiments, these results are not comparable with *in-vivo* needle insertion parameters.

However, perhaps none of the existing models along with *ex-vivo* measurements can accurately assess the forces and tissue deformations while the needle is inserted into the prostate gland through different types of organs and tissues. But, to the best of our knowledge, no *in-vivo* force measurement data for needle insertion in human soft tissue, especially in prostate gland, has been reported. In this study, we have measured and quantified *in-vivo* needle insertion forces and motion profiles during prostate brachytherapy in the OR.

II. MATERIAL AND METHOD

We acquired needle insertion force-torque (F-T) and motion profile data from 25 patients during prostate brachytherapy

1-4244-0033-3/06/$20.00 ©2006 IEEE.

in the OR using a hand-held adapter (Fig. 1 & Fig. 2). The adapter that we have developed is equipped with a 6 DOF force sensor Nano17® (ATI Industrial Automation, Apex, NC) and a 6 DOF electromagnetic (EM)-based position sensor miniBIRD® (Ascension Technology Corporation, Burlington, VT). The miniBIRD® was attached to the hand-held adapter to measure 3D position and orientation of the needle and the corresponding time stamps were recorded automatically for calculating the needle insertion velocity. To have synchronized data, we integrated miniBIRD® with the Nano17® so that force sensor can trigger the position sensor. Additionally, the needle progression into the soft tissue (perineum, prostate and other organs) and prostate deformation and movement were recorded using ultrasound (Acuson™ 128xP, Mountain View, CA) imaging technique.

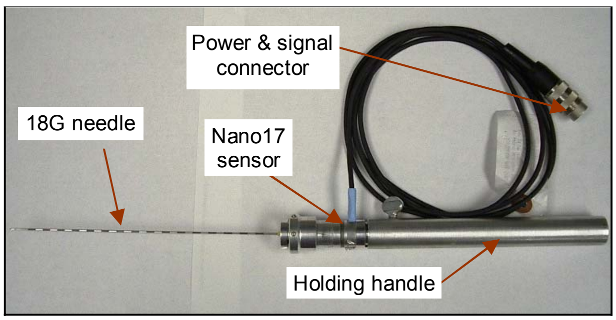

Fig. 1. Hand-held adapter for inserting the needle.

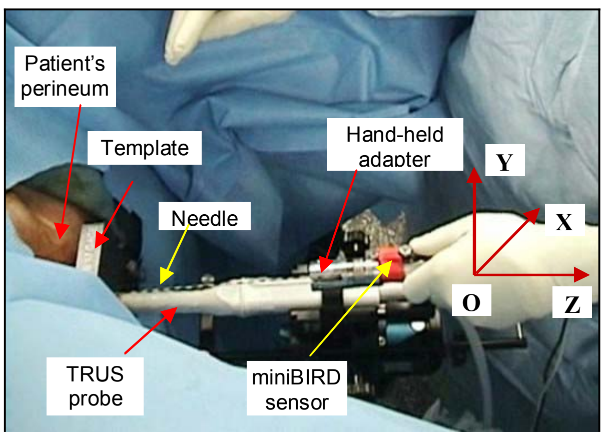

Fig. 2. Force-torque and position data collection during actual brachytherapy procedure in the OR.

Data were collected under a Research Subject Review Board (RSRB) approved protocol and with patient's informed consent. Commercially available brachytherapy needles having 1.47mm (17G) and 1.27mm (18G) in diameter and 200mm in length with diamond tip trocars (Mick Radio-Nuclear instruments, Inc., NY) were used. There were thirty-six 17G needle insertions in 12 patients and thirty-six 18G needle insertions in another 13 patients with 2-3 insertions per patient. Only one type of needle (either 17G or 18G) was used for each of the patients. Of the 25 patients, in 22 patients the hand-held adapter was operated by an experienced surgeon having more than 30 years of surgical experience and 8 years of PSI experience. The other 3 patients were treated by another surgeon having about 3 years of PSI experience. An experienced radiologist captured the TRUS images, in sagittal plane, of the needle progression through various tissues and organs. The time, position, and force data during needle insertion were recorded at a frequency of 100Hz.

III. RESULT AND DISCUSSION

Selection of the needle size (17G or 18G) during a PSI (prostate brachytherapy) procedure is based on certain patient-specific criteria and the physical properties of the needle. For instance, if the patient receives prior hormonal therapy or External Beam Radiation Treatment (EBRT) then the prostate becomes harder which, in turn, requires a stiffer needle to reduce undesirable deviation of the needle from the desired trajectory. The other important criteria are the hardness and thickness of the skin of the patient and special anatomic conditions. The thicker or harder the skin, the stiffer the needle required, therefore, a 17G needle is used because of its larger diameter. However, another option could be the use of stronger material, but no such needle is commercially available or cost prohibitive. Use of an 18G needle is preferable due to the fact that it creates less trauma, edema and tissue/organ deformation or movement. However, the surgeon decides the needle based on the patient's conditions and with informed knowledge of the properties of the needle.

Here, we present a representative case of a single needle insertion force and velocity into one patient for an 18G needle (Fig. 3) and into another patient for 17G needle (Fig. 4). Since, after insertion the needle needs to be in the patient for delivering seeds, we have not presented force data during retraction of the hand-held adapter. From *in-vivo* data of the 18G needle, we observe a sudden increase in insertion (F_z) force when the needle penetrates into the patient's skin (Fig. 3(a)). The force continued to increase until about 25mm of insertion (maximum force is about 14.5N), then decreased partly due to the relaxation in tissue/organ and partly due to the surgeon pausing to confirm the needle penetration from the US image. As the needle hits the prostate capsule (at about 92mm of penetration) the force again increases rapidly and reached a maximum at the point of capsule puncture.

The needle insertion velocity has been calculated using needle position data and recorded time stamps. We observe that the maximum needle insertion velocity at the initial stage is quite high (about 2.0m/s), however, in the later stage of the penetration the velocity decreased significantly with some peaks (Fig. 3(b)). This velocity profile is remarkably different from many robotic needle insertions during *ex-vivo* experiments mainly due to the surgeon's pause to confirm the location of the needle with respect to the target. In the case of a robotic needle insertion into a patient, we may be unable to attain such a high velocity safely. However, we have not noticed any significant difference in measured parameters when the insertion velocities were small (ref. Table 1, for patient #17 v_{max}=0.59m/s, and for patient #19, v_{max}=0.4m/s; these were performed by another surgeon). It appears that at relatively slower speed of needle that is suitable for clinical procedure, the force on the needle may not change significantly. However, requires further study to access the effects of velocity modulation on insertion force and needle placement accuracy in living biological tissues which relax quite fast and to a large amount [5],[11]-[12].

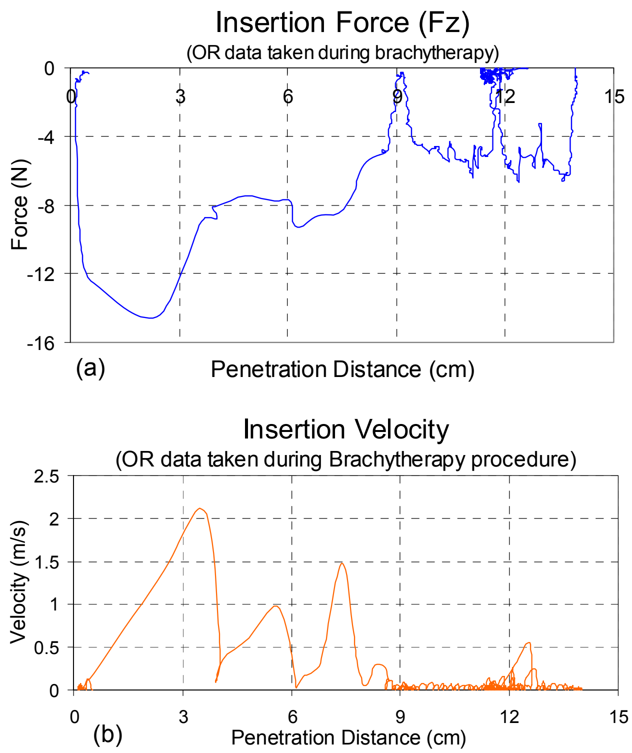

Fig. 3. *In-vivo* measured (a) force and (b) velocity profiles of an 18-gauge (1.27mm) needle for a single insertion into a patient during actual brachytherapy procedures.

A representative data set (a single needle insertion into a patient) for a 17G needle insertion has been presented in Fig. 4, from which we observe similar profiles of force and motion as noticed for the 18G needle. However, the magnitude of insertion force is remarkably high as compared to that of on the 18G needle (Fig. 4 (a)). Here, we observe that for a 17G needle the insertion force is about 17.8N (Fig. 3(a)), whereas on the 18G needle the insertion force is about 14.5N. A significant part of these force differences for two types of needles is attributed to the needle size differences, i.e. 18G (1.27mm) and 17G (1.47mm). However, the velocity profiles for both the needles are similar which indicates consistent style of needle insertion by the surgeon.

A summary of the *in-vivo* data collected from all 25 patients (total 72 insertions) has been presented in Table I. Average maximum forces before and after penetration into the prostate and also average maximum needle velocities have been tabulated here. The insertion force and velocity have been averaged for each patient (parameters were measured for 2-3 insertions per patient) along with the standard deviation (SD). Then for each type of needle (17G or 18G) the measured parameters have been averaged to find the overall mean value. The overall average maximum forces outside and inside the prostate are 7.79N and 6.21N, respectively, for 18G needles (first 13 patients in Table I). We notice a significant reduction of insertion force (about 20% less) when the needle penetrates in the prostate. This reduction in force is mainly due to the presence of softer tissue. On the other hand, for 17G needle the insertion force dropped from 13.75N outside the prostate to 9.20N in the prostate (last 12 patients in Table I), a reduction of about 33%. It indicates that the force difference for 17G needle is more prominent compared to 18G needle.

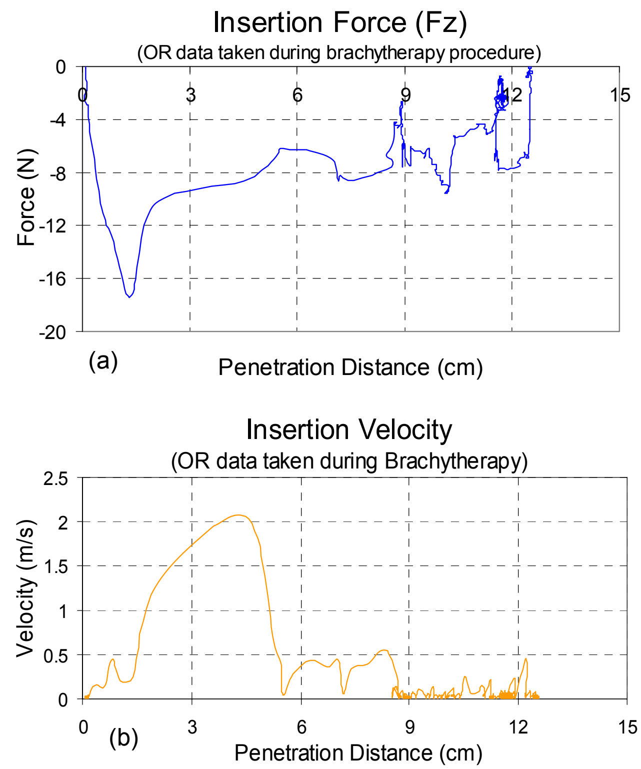

Fig. 4. *In-vivo* measured (a) force and (b) velocity profiles of a 17-gauge (1.47mm) needle for a single insertion into a patient during actual brachytherapy procedures.

A comparison of overall maximum forces on the 18G and 17G needles reveals that the perineum force on the 18G needle is about 43% less and the prostate force is about 32.5% less as compared to that on the 17G needle, suggesting a relatively less prominent effect of needle size in softer tissue. The average maximum velocity of 17G needle (1.43m/s) was higher than that of 18G needle (1.20m/s). This is due to the fact the surgeon anticipated larger force on 17G needle and he tried to thrust the needle faster to compensate it. However, the effect of higher velocity does not appear to have a significant effect on insertion force as seen in Table 1, for subject #17 (v_{max}=0.59m/s) and patient #19 (v_{max}=0.4m/s), which were performed by another surgeon who inserted the needles slowly and gradually.

IV. CONCLUSION AND FUTURE WORK

In this paper, we presented *in-vivo* force-torque and needle insertion motion profile data collected from 25 patients during actual brachytherapy procedure in the OR. The force data has been collected using a 6 DOF force sensor. The needle position has been recorded using a 6 DOF EM-based sensor. The *in-vivo* data reveals that maximum average needle insertion force for 18G needle is significantly lower (about 7.8N/6.2N) as compared to that of 17G needle

(13.8N/9.2N); the maximum average insertion velocity of 17G needle is higher (1.44m/s) as compared to that of 18G needle (1.2m/s). A second surgeon inserted needles at a slower speed (about 0.5m/s) to perform multiple cases from which it appears that the velocity of needle insertion has minimal effect on the force. However, we are further investigating the effect of velocity modulation on needle insertion. For safety reasons, if the surgeon chooses to operate the robot at a lower speed, the amount of force on the needle is expected to remain within the measured range.

It is intuitive that lower force will cause less deformation and displacement of internal tissue/organ, and create less trauma and edema to the patients. Thus, use of 18G needle (1.27mm in diameter) is more logical from a clinical point of view. However, 17G needle (1.47mm in diameter) is used based on some unavoidable patient-specific criteria for some patients who have undergone other treatments such as hormonal therapy, EBRT, etc. which makes the prostate harder and patients with thicker and stiffer skins.

The collected *in-vivo* data imparts useful insights into the force on the needle, and needle velocity during actual brachytherapy procedure in the OR. This information will provide guidance in the design and control of a robotic system for prostate brachytherapy treatment with implantable radioactive seeds. The acquired knowledge also can be quite useful in developing predictive deformation model of the prostate and real-time adaptive control of the needle.

TABLE I
IN-VIVO FORCE AND VELOCITY

Needle	Subject	Max. Force in Perineum (N) (Avg./SD)	Max. Force in Prostate (N) (Avg./SD)	Max. Vel. (m/s) (Avg./SD)
18G (1.27mm) diamond tip	Sub. #3	5.22/0.54	6.06/0.18	0.88/0.06
	Sub. #4	7.90/1.20	6.65/0.01	0.73/0.24
	Sub. #5	8.75/0.42	8.41/1.59	1.78/0.84
	Sub. #8	9.80/2.01	8.15/3.17	2.08/0.36
	Sub. #9	3.41/1.33	4.69/1.29	1.49/0.81
	Sub. #11	5.58/0.64	6.26/1.45	0.79/0.19
	Sub. #14	6.15/5.99	6.06/3.35	1.95/1.10
	Sub. #17	9.45/5.18	0.55/0.46	0.59/0.26
	Sub. #18	10.71/6.29	5.32/1.32	0.92/0.63
	Sub. #19	6.50/3.95	5.51/0.94	0.40/0.29
	Sub. #20	9.90/4.01	5.10/1.11	1.54/0.49
	Sub. #22	8.46/0.93	5.91/2.27	0.98/0.31
	Sub. #23	7.32/3.36	6.8/1.46	1.25/0.55
	13 Patients	**7.79/3.45**	**6.21/1.74**	**1.20/0.71**
17G (1.47mm) diamond tip	Sub. #1	13.85/5.31	8.28/1.2	0.61/0.42
	Sub. #2	16.85/4.45	8.85/4.74	1.17/0.4
	Sub. #6	11.73/1.69	9.62/5.58	0.94/0.16
	Sub. #7	11.48/0.69	5.43/1.04	0.70/0.47
	Sub. #10	14.23/4.02	8.11/1.40	0.86/ 0.08
	Sub. #12	12.69/4.88	9.54/1.09	1.61/0.27
	Sub. #13	13.89/1.10	11.14/2.62	1.27/0.36
	Sub. #15	13.66/4.71	8.14/2.17	1.67/0.74
	Sub. #16	14.76/2.19	9.42/0.32	1.61/0.41
	Sub. #21	15.67/4.55	9.01/0.18	2.27/2.10
	Sub. #24	16.7/1.23	8.71/3.0	1.65/0.84
	Sub. #25	9.83/1.24	7.24/1.69	2.4/1.05
	12 Patients	**13.75/3.40**	**9.20/3.70**	**1.43/0.69**

ACKNOWLEDGEMENT

This work is supported by the National Cancer Institute, under grant R01 CA091763. We would like to thank Dr. Ganesh Palapattu, Ms. Maureen Kiernan, Ms. Kim Ferrari, and Ms. Suzanne Vandeursen, and other clinical staff who helped us in collecting data in the OR.

REFERENCE

[1] G. Fichtinger, T.L. DeWeese, A. Patriciu, A. Tanacs, D. Mazilu, J.H. Anderson, K. Masamune, R. Taylor, and D. Stoianovici, "System for Robotically Assisted Prostate Biopsy and Therapy with Intraoperative CT Guidance," in the Journal Acad. Rad., Vol. 9, pp. 60-74, 2002.

[2] Z. Wei, G. Wan, L. Gardi, D.B. Bowney, and A. Fenster, "Robotic Aided 3D TRUS Guided Intraoperative Prostate Brachytherapy," in the *Proc. of SPIE*, Vol. 5367, pp. 361-370, Bellingham, WA, 2004.

[3] Y. Yu, T.K. Podder, Y. Zhang, W.S. Ng, J. Sherman, D. Fuller, V. Misic, L. Fu, E.M. Messing, D.J. Rubens, J.G. Strang, and R. A. Brasacchio, "Robot-assisted Prostate Brachytherapy," in the *Int. Conf. on Medical Image Computing and Computer Assisted Intervention (MICCAI)*, Copenhagen, Denmark , (accepted), 2006.

[4] P.L. Williams, and R. Warwick, "*Gray's Anatomy*," 38th Edition, edited by L. H. Bannister, *et al*., Churchill Livingstone Company, New York, 1995.

[5] Y.C. Fung, "*Biomechanics: Mechanical Properties of Living Tissues*," 2nd Edition, Springer-Verlag, New York, 1993.

[6] T.A. Kruoskop, T.M. Wheeler, F. Kaller, B. S. Garra, and T. Hall, "Elastic Moduli of Breast and Prostate Tissues under Compression," in the Journal of Ultrasonic Imaging, Vol. 20, pp. 260-274, 1998.

[7] P.S. Wellman, R.D. Howe, E. Dalton, and K.A. Kern, "Breast Tissue Stiffness in Compression is Correlated to Histological Diagnosis," *Technical Report, Harvard BioRobotics Laboratory*, Division of Engineering and Applied Science, Harvard University, 1999.

[8] I. Sakuma, Y. Nishimura, *et al*., "In Vitro Measurement of Mechanical Properties of Liver Tissue under Compression and Elongation using a New Test Piece Holding Method with Surgical Glue," in *the IS4TM/LNCS*, Vol. 2673, pp. 223-230, 2003.

[9] A. Samani, J. Bishop, C. Luginbuhl, and D. B. Plewes, "Measuring the Elastic Modulus of ex-vivo small Tissue Samples," in the *Journal of Phy. in Med. and Bio.*, Vol. 48, No. 4, pp. 2183-2198, 2003.

[10] K. Matsumiya, Y. Momoi, E. Kobayashi, *et al*., "Analysis of Forces during Robotic Needle Insertion to Human Vertebra," in *the MICCAI (LNCS*, Vol. 2878, pp. 271-278), Montreal, Canada, Nov. 2003.

[11] T.K. Podder, D.P. Clark, D. Fuller, J. Sherman, W.S. Ng, L. Liao, D.J. Rubens, J.G. Strang, E.M. Messing, Y.D. Zhang, and Y. Yu, "Effects of Velocity Modulation during Surgical Needle Insertion," in the *Proceedings of the 27th Annual International Conference of the IEEE Engineering in Medicine and Biology Society (EMBS),* pp. 6766-6770, Shanghai, China, Sept. 2005.

[12] T.K. Podder, L. Liao, J. Sherman, V. Misic, Y.D. Zhang, D. Fuller, D.J. Rubens, E.M. Messing, J.G. Strang, W.S. Ng, and Y. Yu, "Assessment of Prostate Brachytherapy and Breast Biopsy Needle Insertions and Methods to Improve Targeting Accuracy," in the *IFMBE Proceedings of the 12th International Conference on Biomedical Engineering (ICBME)*, Vol. 12, Singapore, Dec. 2005.